



# Aggregation and Crosslinking of Poly(*N,N*-dimethylacrylamide)-*b*-pullulan Double Hydrophilic Block Copolymers

Alexander Plucinski, Jochen Willersinn, Rafael B. Lira, Rumiana Dimova,\* and Bernhard V. K. J. Schmidt\*

The self-assembly of polymers is a major topic in current polymer chemistry. In here, the self-assembly of a pullulan based double hydrophilic block copolymer, namely pullulan-*b*-poly(*N,N*-dimethylacrylamide)-*co*-poly(diacetone acrylamide) (Pull-*b*-(PDMA-*co*-PDAAM)) is described. The hydrophilic block copolymer induces phase separation at high concentration in aqueous solution. Additionally, the block copolymer displays aggregates at lower concentration, which show a size dependence on concentration. In order to stabilize the aggregates, crosslinking via oxime formation is described, which enables preservation of aggregates at high dilution, in dialysis and in organic solvents. With adequate stability by crosslinking, double hydrophilic block copolymer (DHBC) aggregates open pathways for potential biomedical applications in the future.

poly(butadiene)-*b*-poly(ethylene oxide) (PB-*b*-PEO). A significant drawback for the application of polymersomes in biomedical applications, is their poor biocompatibility and the insufficient permeability of the hydrophobic part of the polymersome membrane.<sup>[11]</sup> An alternative route to form aggregates, is to use pure hydrophilic block copolymers, e.g., double hydrophilic block copolymers (DHBCs).<sup>[12]</sup> In literature, the most common strategy to form aggregates of DHBCs in aqueous solution is to operate with an external trigger. Therefore, one of the hydrophilic blocks turns hydrophobic after external perturbation, which could be tempera-

## 1. Introduction

Self-assembly of block copolymers is an important feature for applications of polymers,<sup>[1,2]</sup> which especially counts toward applications in the area of drug delivery and release systems,<sup>[3,4]</sup> nano reactors<sup>[5]</sup> or tissue engineering.<sup>[6]</sup> Frequently used are aggregates like micelles<sup>[7]</sup> or vesicles<sup>[8]</sup> that are formed from amphiphilic block copolymers. Vesicles formed by amphiphilic block copolymers are called polymersomes,<sup>[9,10]</sup> e.g., from

temperature<sup>[13,14]</sup> or pH change for example.<sup>[13]</sup> While external triggers allow the formation self-assembled structure of DHBCs, still the hydrophobic effect drives aggregate formation. In order to circumvent the disadvantages of polymersomes, a different way of self-assembly needs to be introduced. For polymersomes made of amphiphilic polymers, the aggregation results from the hydrophobic effect, while the aggregation for the pure hydrophilic DHBCs can be established via the different degree of hydrophilicity of the different blocks.<sup>[15,16]</sup> Complete water soluble DHBCs shown self-assembled structures in aqueous environment as well that are formed of DHBCs with specially chosen block combinations in aqueous systems at high concentration. At lower concentration, the formed self-assembled structures are breaking down. The aggregation of DHBCs can be understood from the perspective of aqueous multiphase systems that feature phase separation of homopolymer mixtures in water at elevated concentration.<sup>[17–20]</sup> The different hydrophilic blocks of the DHBC are bound covalently. Due to the different osmotic pressure and Laplace pressure, in the hydrophilic polymer domains, the system needs to demix on the microscopic scale to compensate the various pressures.<sup>[21,22]</sup> For a stable aggregate formation, both pressures should be equal. For the self-assembly of DHBCs, the polymer-polymer interaction has a significant influence. According to the studies by Brosnan et al.,<sup>[23]</sup> the different hydrophilicity of the chosen polymer blocks needs to be significant, to form a stable self-assembled structures. In the realm of block copolymers, earlier studies have shown that block copolymers like PEO-*b*-poly(2-methyl-2-oxazoline),<sup>[24,25]</sup> PEO-*b*-poly(*N,N*-dimethylacrylamide)

A. Plucinski, Dr. J. Willersinn, Dr. R. B. Lira, Dr. R. Dimova,  
Dr. B. V. K. J. Schmidt  
Max Planck Institute of Colloids and Interfaces  
Am Mühlenberg 1, Potsdam 14476, Germany  
E-mail: rumiana.dimova@mpikg.mpg.de;  
bernhard.schmidt@glasgow.ac.uk

A. Plucinski, Dr. B. V. K. J. Schmidt  
School of Chemistry  
University of Glasgow  
Glasgow G12 8QQ, UK

Dr. R. B. Lira  
Moleculaire Biofysica  
Zernike Instituut Rijksuniversiteit Groningen  
Groningen, Netherlands

The ORCID identification number(s) for the author(s) of this article can be found under <https://doi.org/10.1002/macp.202000053>.

© 2020 The Authors. Published by WILEY-VCH Verlag GmbH & Co. KGaA, Weinheim. This is an open access article under the terms of the Creative Commons Attribution License, which permits use, distribution and reproduction in any medium, provided the original work is properly cited.

DOI: 10.1002/macp.202000053

(PEO-*b*-PDMA)<sup>[26]</sup> or PEO-*b*-poly(2-(methacryloyloxy)ethyl phosphorylcholine)<sup>[22]</sup> show microphase separation and aggregate formation in aqueous environment. The research of Brosnan et al.<sup>[23]</sup> showed the formation of aggregates by different combinations of hydrophilic blocks, i.e., dextran-*b*-PEO, pullulan-*b*-PEO, and dextran-*b*-poly(sarcosine), present in aqueous solution at high concentration (15–25 wt%). Continuing research indicated the self-assembly behavior of other DHBCs at lower concentration, e.g., poly(2-ethyl-2-oxazoline)-*b*-poly(*N*-vinylpyrrolidone) (PEtOx-*b*-PVP),<sup>[27]</sup> PEO-*b*-PEtOx,<sup>[28]</sup> pullulan-*b*-PVP<sup>[29]</sup> or pullulan-*b*-PDMA.<sup>[30]</sup> Especially glyco polymers were investigated regarding DHBC self-assembly frequently<sup>[31–34]</sup> for example poly(2-hydroxyethyl methacrylate)-*b*-poly(2-*O*-(*N*-acetyl- $\beta$ -D-glucosamine)ethyl methacrylate).<sup>[31]</sup>

In order to investigate novel polysaccharides-based DHBCs, pullulan (Pull) is a good choice as a biocompatible block.<sup>[35]</sup> This linear biopolymer consists of maltotriose units coupled via 1,6- $\alpha$ -bonds.<sup>[36]</sup> Pullulan is a well-known biopolymer, which is applied in biomedicine,<sup>[36–38]</sup> e.g., blood plasma substitutes<sup>[39]</sup> or as a carrier for gene delivery.<sup>[40,41]</sup> In addition, pullulan shows an interesting aggregation behavior in combination with poly(acrylamides), e.g., PDMA.<sup>[30]</sup>

The synthesis of DHBCs can be conducted via reversible addition–fragmentation chain transfer (RAFT) polymerization.<sup>[42]</sup> An alternative route to form DHBCs is via copper catalyzed alkyne–azide cycloaddition (CuAAC) (1,3-dipolar cycloaddition) first described by Huisgen et al.<sup>[43]</sup> and comparatively by Kolb and Sharpless described as click chemistry,<sup>[44]</sup> which could also be used for the preparation of various macromolecular architectures.<sup>[45,46]</sup> For the formation of a novel block copolymer, one homopolymer needs to be alkyne end-functionalized and the second polymer should be azido end-functionalized. One route to form alkyne end-functionalized polymer is to functionalize bio-based polymers, e.g., pullulan<sup>[47]</sup> or synthetic polymers, e.g., poly(2-hydroxyethyl methacrylate) (PHEMA)<sup>[48]</sup> with an alkyne end group. For hydrophilic azido end-functionalized polymers, RAFT polymerization<sup>[49]</sup> is a technique to synthesize functionalized poly(acrylamides), e.g., PDMA.<sup>[50]</sup> Consequently, a large pool of possible block copolymer combinations formed by CuAAC is available. Starting from a small number of building blocks, it is possible to form a significant number of different block copolymers.

An important requirement for a future application of DHBC aggregates is a high stability. One way to improve stability is crosslinking of the DHBCs aggregates.<sup>[51]</sup> For pullulan based DHBCs, crosslinking of the pullulan block was investigated in the past to improve aggregate stability in aqueous solution, e.g., via sodium trimetaphosphate (STMP)<sup>[52]</sup> or via cystamine forming dynamic covalent imine linkages with aldehyde groups after pullulan oxidation.<sup>[29]</sup> Moreover, there are many different options from supramolecular chemistry to crosslink DHBCs, e.g., via hydrogen bonds or host-guest inclusion complexes.<sup>[53,54]</sup> An alternative method for crosslinking of polymers is the reaction of primary amines or hydroxylamine with aldehydes or ketones to generate an oxime or imine bond, which was used to form biocompatible hydrogels.<sup>[55]</sup> As such, the formation of a reversible oxime bond is an efficient technique to modify the structure of macromolecules.<sup>[56,57]</sup> For example, oxime formation was used by Sumerlin and co-workers for the crosslinking of polymers containing diacetone acrylamide (DAAM) as repeating unit in aqueous solution.<sup>[58]</sup>

Herein, the self-assembly behavior of the DHBC Pull-*b*-(PDMA-*co*-PDAAM) in aqueous environment is investigated. Toward this end, alkyne end-functionalized pullulan is coupled via CuAAC with an azide end-functionalized PDMA-*co*-PDAAM. Subsequently, Pull-*b*-(PDMA-*co*-PDAAM) is analyzed via <sup>1</sup>H-NMR, <sup>13</sup>C-NMR spectroscopy, and size exclusion chromatography (SEC). Additionally, the Pull-*b*-(PDMA-*co*-PDAAM) is crosslinked via oxime formation (**Scheme 1**), which is investigated via <sup>1</sup>H-NMR and <sup>13</sup>C-NMR spectroscopy. Moreover, the aggregation behavior of Pull-*b*-(PDMA-*co*-PDAAM) and crosslinked Pull-*b*-(PDMA-*co*-PDAAM) is analyzed via cryo SEM, dynamic light scattering (DLS), and confocal laser scanning microscopy (CLSM). Additionally, the behavior of the aggregates in the organic solvent *N*-methyl-2-pyrrolidone (NMP) is studied as well.

## 2. Results and Discussion

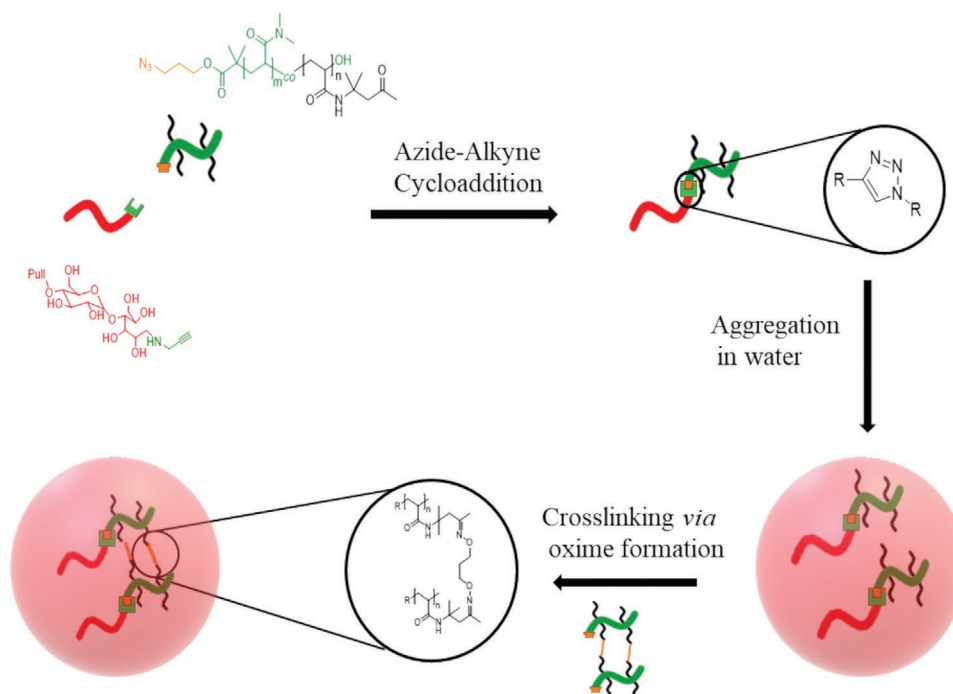
### 2.1. Synthesis of PDMA-*co*-PDAAM

Copolymers like PDMA-*co*-PDAAM are easily formed via reversible deactivation radical polymerization, e.g., RAFT polymerization. Dodecylthiocarbonylthio-2-methylpropanoic acid 3'-azido propyl ester was used as chain transfer agent based on a procedure, known from literature.<sup>[50]</sup> The ratio between DMA and DAAM was adjusted to 1:4, to introduce a ratio of 20% of DAAM in the final copolymer. PDMA-*co*-PDAAM was obtained as copolymer with molar mass of 27 800 g mol<sup>-1</sup> and a  $\bar{D}$  of 1.9. The presence of both monomers in the azido functionalized polymer was proven by <sup>1</sup>H-NMR spectroscopy that shows the peaks for PDMA and PDAAM at 3.0 and 2.1 ppm. The integral ratio between the peak at 3.0 ppm for the two methyl groups (PDMA) and the terminal single methyl group (PDAAM) at 2.1 ppm is around 8:1. According to the integration the content of PDAAM is 20% (Figure S3, Supporting Information).

The azido functional group was introduced to react with alkyne end-functionalized pullulan. In order, to avoid side reactions in the following CuAAC reaction and side effects caused by hydrophobic moieties during self-assembly, the RAFT-group was converted to a hydroxyl group. For that, the PDMA-*co*-PDAAM was reacted with tetrahydrofuran peroxide and ascorbic acid.<sup>[59,60]</sup> Finally, azido functionalized PDMA-*co*-PDAAM was obtained with a molar mass of 22 000 g mol<sup>-1</sup> and  $\bar{D}$  of 1.9 (Table S1, Supporting Information). Moreover, the hydroxy functionalized copolymer was characterized via <sup>1</sup>H-NMR.

### 2.2. Synthesis of Pullulan-*b*-(PDMA-*co*-PDAAM) via Copper Catalyzed Azide Alkyne Cycloaddition

CuAAC is an alternative avenue to form new block copolymers.<sup>[43]</sup> First, pullulan was depolymerized in an aqueous hydrochloric acid solution and end functionalized in an acetate buffer solution via reductive animation of the aldehyde end-group of the pullulan, using propargyl amine and sodium cyanoborohydride. The kinetic of the depolymerisation of pullulan can be controlled with the temperature of the reaction



**Scheme 1.** Schematics of the formation of pullan-*b*-poly(*N,N*-dimethylacrylamide)-*co*-poly(diacetone acrylamide) (Pull-*b*-(PDMA-*co*-PDAAM)) via copper catalyzed azide-alkyne cycloaddition (CuAAC), the self-assembly process in water toward droplet formation and crosslinking via oxime formation.

and concentration of the acid.<sup>[61]</sup> To ensure full conversion to the pullulan alkyne, a significant excess of sodium cyanoborohydride was used.<sup>[62]</sup> The alkyne end-functionalized pullulan was analyzed via <sup>1</sup>H-NMR (Figure S2, Supporting Information). Due to the overlapping of the propargyl proton and protons of the pullulan, the alkyne could not be detected directly via <sup>1</sup>H-NMR. However, the absence of the anomeric protons of pullulan ( $\beta$ -form 6.3 and  $\alpha$ -form 6.7 ppm), is an indicator for the conversion of the pullulan end-group. Azido end-functionalized PDMA-*co*-PDAAM and alkyne end-functionalized pullulan were conjugated under copper catalysis via a triazole as linker (Scheme 1).<sup>[47]</sup> For the cycloaddition of two hydrophilic block copolymers, the reaction was carried out in a mixture of DMSO and water. To ensure the full conversion of the reaction, an excess of alkyne end-functionalized pullulan was present. Azide functionalized PS-resin was added after the reaction to bind unreacted pullulan. After the reaction the PS-resin was removed easily.

The formed block copolymer was analyzed via SEC, DOSY-NMR, <sup>1</sup>H-NMR, and <sup>13</sup>C-NMR (Figure 1 and Figure S4, Supporting Information). <sup>1</sup>H-NMR and <sup>13</sup>C-NMR show the presence of pullulan and PDMA-*co*-PDAAM in the copolymer, e.g., the signal from protons of pullulan around 3.4 to 3.7 ppm, the signal from the two methyl groups of PDMA around 3.0 ppm and terminal methyl group of the PDAAM around 2.1 ppm. In order to prove the successful block copolymer formation, the block copolymer was analyzed via DOSY-NMR. The DOSY-NMR measurement (Figure 1c) showed two species. A species with high diffusion coefficient originating from the solvent d-DMSO and artefact from the solvent around  $9 \times 10^{-6} \text{ cm}^2 \text{ s}^{-1}$ . In DOSY-NMR, very strong gradient pulses may result in artefacts.<sup>[63]</sup> The second species, at a lower diffusion coefficient ( $8 \times 10^{-7} \text{ cm}^2 \text{ s}^{-1}$ )

included all <sup>1</sup>H-NMR peaks, from the individual blocks in the block copolymer, which confirms block copolymer formation. Moreover, SEC measurements indicate block copolymer formation via a shift in the elugram toward shorter retention times. Additionally, a comparison of elugrams between Pull-*b*-PDMA-*co*-PDAAM and the mixture of pullulan and PDMA-*co*-PDAAM showed a significant difference. According to pullulan calibration a molar mass of  $25\,800 \text{ g mol}^{-1}$  was obtained (Figure 1b and Table S1, Supporting Information).

### 2.3. Phase Separation of Pull-*b*-(PDMA-*co*-PDAAM) in Aqueous Solution

Aggregation of DHBCs in aqueous solution without external triggers, such as pH change or temperature, demand specific properties of block copolymers and particular conditions. One of the most important conditions is concentration.<sup>[12,24,25]</sup> In order to analyze the aggregation of Pull-*b*-(PDMA-*co*-PDAAM), a 20 wt% solution was investigated via CSLM, which revealed the presence of mesoscopic polymer enriched droplets in water (Figure 2b and Figure S8b, Supporting Information). The 20 wt% polymer solution was observed under bright field (Figure 2e) and CLSM with SRB as additive. In both cases, the presence of polymer droplets in a polymer/water matrix with sizes between 10 and 50  $\mu\text{m}$  is visible on the time scale of the experiment. In order to investigate the position of the polymer, the polymer was labelled, and the concentrated solution was analyzed via CLSM (Figure 2a). The image with the labelled polymer displays a higher concentration of the polymer in the droplet, indicating that the polymer is enriched in this phase, which hints the continuous distribution of the fluorescently

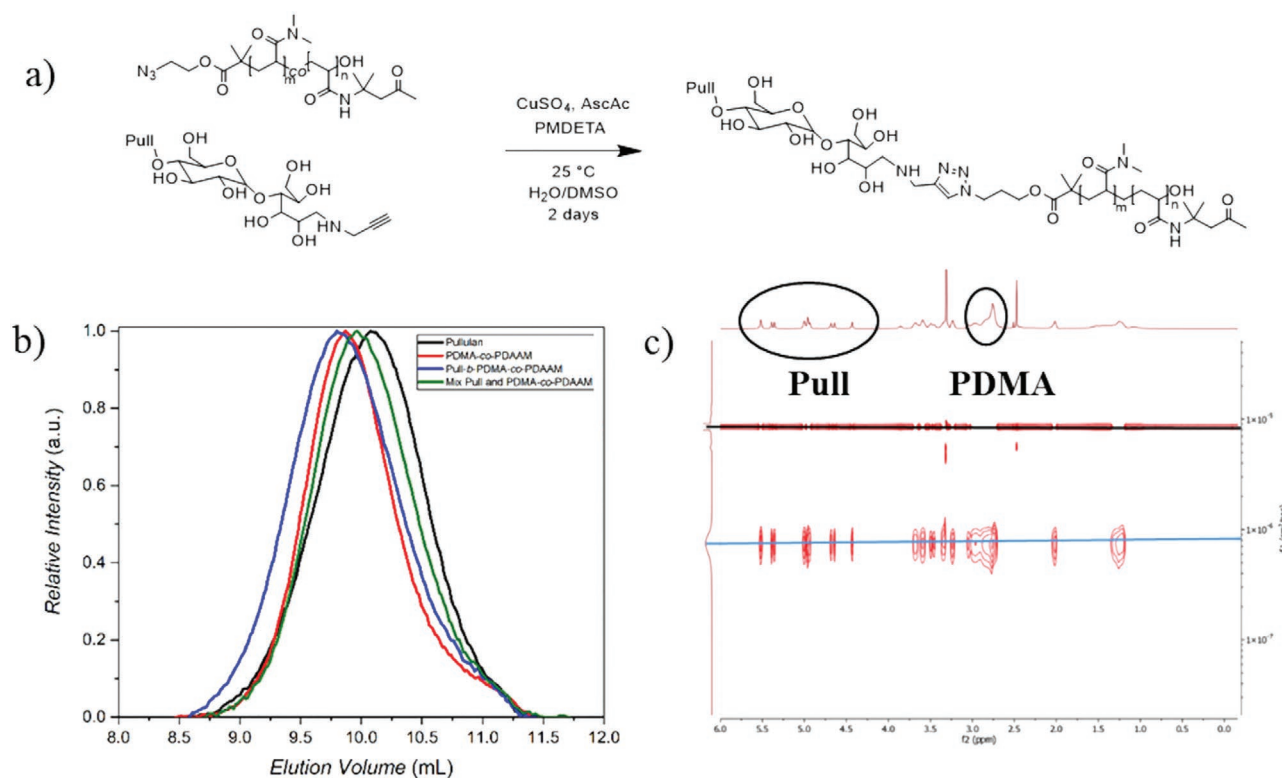


**Figure 1.** a) Reaction scheme for the formation of Pull-*b*-(PDMA-*co*-PDAAM), b) SEC measurement of depolymerized pullulan (black curve), PDMA-*co*-PDAAM (red curve), mixture of depolymerized pullulan and PDMA-*co*-PDAAM (green curve), and Pull-*b*-(PDMA-*co*-PDAAM) (blue curve) measured in acetate buffer against pullulan standards, c) DOSY measurement of Pull-*b*-(PDMA-*co*-PDAAM) (measured in DMSO-*d*<sub>6</sub>) with the diffusion coefficient of DMSO-*d*<sub>6</sub> (black line) and Pull-*b*-(PDMA-*co*-PDAAM) including all <sup>1</sup>H-NMR peaks, from all individual blocks (blue line).

labelled polymer and demonstrates droplet formation. Note that similar objects have been reported in the literature on DHBC self-assembly and referred to as giant vesicles,<sup>[23]</sup> which might need reconsideration based on our results

Interestingly, the phases can be inverted as well, e.g., at high concentration two kinds of droplets were shown via CSLM: In one case the polymer is more concentrated in the droplet, in the other case the polymer is more concentrated in the continuous phase outside the droplet (Figure 2d and Figure S5, Supporting Information). In all CLSM measurements, both cases were observed, the polymer outside and inside the droplet. The result of inverted droplets indicates that the formation of polymer-rich droplets in water or water in polymer-rich matrix is a very sensitive system, which is currently investigated in detail in our laboratory.<sup>[64]</sup> However, the droplets are only stably formed at high polymer concentrations. Notice that the phases are metastable; upon contact, the droplets fuse, demonstrating their liquid-like behavior. Upon dilution with water, the droplets destabilize, until they start to dissolve (around 15 wt%) (Figure 2c and Figure S8a, Supporting Information). Therefore, concentrations between 15 and 20 wt% were employed for the CLSM measurement. Above 20 wt% the solution is very viscous and was not studied. Below 15 wt% no droplets were present (Figure 2c).

In order to investigate the aggregation behavior of Pull-*b*-(PDMA-*co*-PDAAM) in aqueous solution at lower concentrations, the aqueous solution was analyzed by DLS at 25 °C.

Therefore, 5.0, 2.5, 1.25, 0.6, and 0.1 wt% solution of Pull-*b*-(PDMA-*co*-PDAAM) block copolymer was prepared and analyzed to determine apparent hydrodynamic radii ( $R_{app}$ ) for the formed aggregates at each concentration (Figure S6, Supporting Information). At higher concentration DLS does not deliver reliable results. The intensity weighted particle size distribution of Pull-*b*-(PDMA-*co*-PDAAM) shows a dependency on concentration (Table S2, Supporting Information). At all concentrations, bi- or trimodal particle size distributions are observed. The first peak lies around 4 nm for all concentrations, which can be assigned to free polymer chains in the solution.<sup>[24]</sup> The hydrodynamic radius, calculated via DOSY diffusion coefficient, is 1.3 nm, which corresponds to the size of an unimer. The calculated hydrodynamic radius is smaller in comparison to the measured  $R_h$  via DLS (4.2 nm). One reason for the different  $R_h$  might be the solvent. The DOSY-NMR was conducted in *d*-DMSO and the DLS was carried out in H<sub>2</sub>O. For higher concentration, the intensity of small components around 4 nm is lower. The main peak is above 100 nm at all concentrations. The peak over 100 nm indicates the formation of larger aggregates by Pull-*b*-(PDMA-*co*-PDAAM). The size of these larger particles depends on the block copolymer concentration, i.e., the aggregate size increases with increasing concentration. It should be noted though that the mentioned results are extracted from intensity weighted particle size distributions that overestimate larger structures. The 0.6 wt% solution was analyzed via cryo SEM, to investigate the aggregate

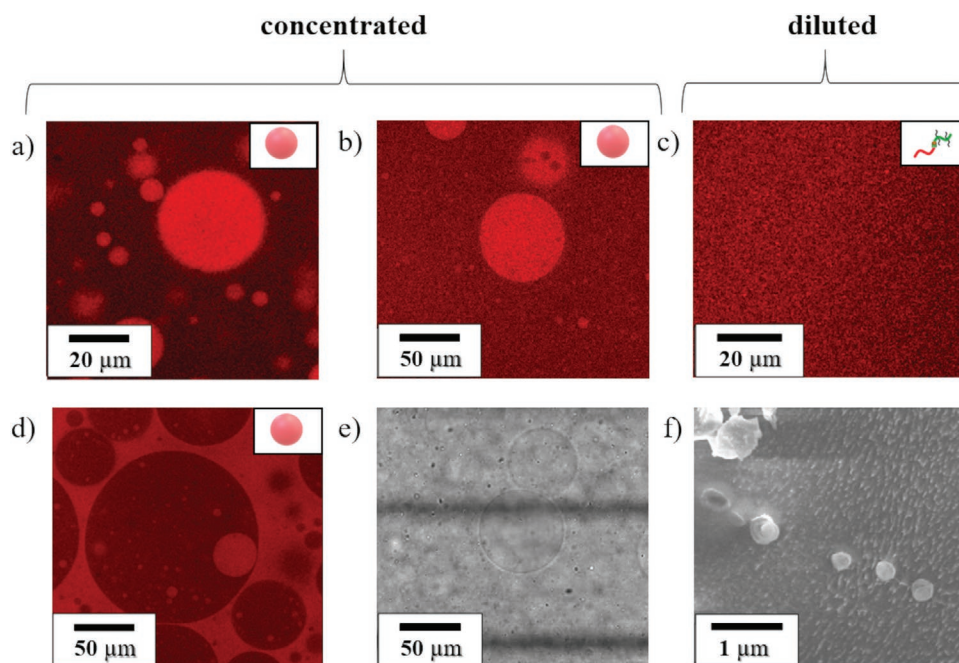


**Figure 2.** a–e) CLSM images of Pull-*b*-(PDMA-*co*-PDAAM): a) mixture of Pull-*b*-(PDMA-*co*-PDAAM) and RhB labelled Pull-*b*-(PDMA-*co*-PDAAM) at 20 wt%, b) Pull-*b*-(PDMA-*co*-PDAAM) at 20 wt% stained with Sulforhodamine B (SRB), c) Pull-*b*-(PDMA-*co*-PDAAM) at 15 wt%, d) inverse phase of Pull-*b*-(PDMA-*co*-PDAAM) at 20 wt% stained with SRB, e) bright field images of Pull-*b*-(PDMA-*co*-PDAAM) at 20 wt%, f) cryo SEM images of Pull-*b*-(PDMA-*co*-PDAAM) at 0.6 wt%.

structure at low concentration. The cryo SEM images of 0.6 wt% solution of Pull-*b*-(PDMA-*co*-PDAAM) display a significant amount of spherical aggregates with a particle size between 200 and 600 nm (Figure 2f). For a concentration of 0.6 wt% of block copolymer, the apparent average hydrodynamic radius was around 165 nm as determined by DLS, which is in the area of the observed diameter by cryo SEM measurements. From the cryo SEM images, the average particle size in 0.6 wt% solution was calculated and confirmed the DLS results. A particle size calculation of 50 particles, revealed an average particle size is 355 nm with standard deviation of 165 nm for the block copolymer Pull-*b*-(PDMA-*co*-PDAAM) (Figure S9, Supporting Information).

#### 2.4. Crosslinking of Pullulan-*b*-(PDMA-*co*-PDAAM) via Oxime Formation

To improve the stability of the phase separated system during dilution and at lower concentration, crosslinking of Pull-*b*-(PDMA-*co*-PDAAM) was considered. An avenue to crosslink Pull-*b*-(PDMA-*co*-PDAAM) is the click reaction of aldehydes or ketones with primary amines or hydroxylamines to generate imine or oxime bonds, respectively (Figure 3a).<sup>[58,65]</sup> As such, the carbonyl group of the DAAM repeating units is a position for crosslinking via oxime formation with a suitable dihydroxylamine. Therefore, the block copolymer was dissolved in water, at a concentration of 20 wt%, the cross linker a hydroxylamine dihydrochloride, 3,5-diaminobenzoic acid dihydrochloride (DABA) as a catalyst,<sup>[65]</sup> and a base namely triethylamine were added. The ratio between keto groups and crosslinker

was adjusted to [keto]: [crosslinker] 2:1, as the crosslinker, 1,3-bis(aminoxy)propane dihydrochloride can react with two keto groups of Pull-*b*-(PDMA-*co*-PDAAM) in order to form a crosslinking point. The oxime is formed by direct condensation of the hydroxylamine with the carbonyl group of the PDAAM at 35 °C.

Oxime formation was investigated via <sup>1</sup>H-NMR (Figure 3c) and <sup>13</sup>C-NMR (Figure S4, Supporting Information) at first. For <sup>1</sup>H-NMR, the presence of the crosslinker is indicated with the typical signal around 1.7–2.0 ppm. Moreover, in <sup>13</sup>C-NMR, the switch of the quaternary carbon with two methyl groups in PDAAM from about 52 to 42 ppm after crosslinking is visible, which indicates that the oxime formation was successful, and the product is not a mixture of block copolymer and crosslinker. Furthermore, the carbonyl group at 220 ppm is not clearly visible after crosslinking. Additionally, the carbons of the crosslinker are observable around 30 to 32 ppm. Overall, the analytical results of the hydroxylamine-treated Pull-*b*-(PDMA-*co*-PDAAM) are similar to the results for oxime crosslinking, in literature.<sup>[58]</sup> For a successful oxime formation, the ratio of DAAM to DMA in the copolymer PDMA-*co*-PDAAM should be high enough, which was determined to be 20%. For a content of 10% and 5% PDAAM in the block copolymer, successful oxime formation could not be verified, for example via <sup>1</sup>H- and <sup>13</sup>C NMR measurement (Figure S5, Supporting Information).

After the verification of the formation of oximes via addition of dihydroxyl amines, in the next step the actual formation of crosslinked structures was investigated. Initially, CLSM showed mesoscale phase separation similar to pure Pull-*b*-(PDMA-*co*-PDAAM) DHBC. For the 20 wt% solution of crosslinked copolymer, droplets (between 10 and 50 μm) are present and

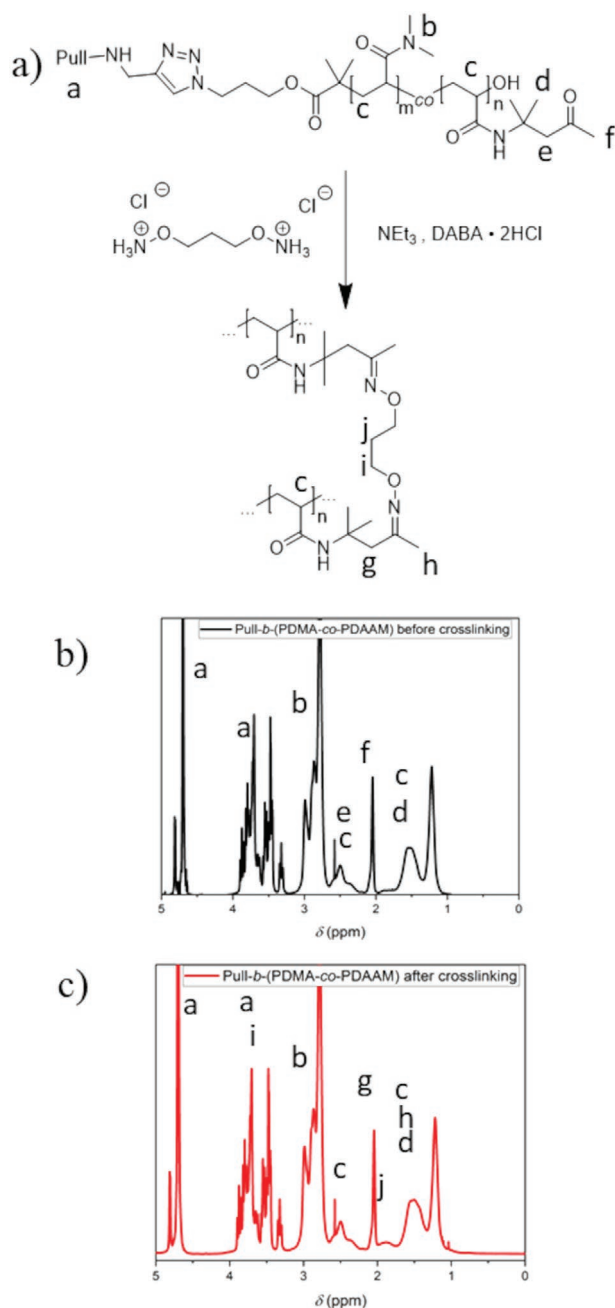


**Figure 3.** a) Reaction scheme for crosslinking of Pull-*b*-(PDMA-*co*-PDAAM) with 1,3-bis(aminoxy)propan dihydrochloride via oxime formation in water employing DABA as catalyst, b) <sup>1</sup>H-NMR before and c) after crosslinking in D<sub>2</sub>O.

visible in bright field (Figure S10, Supporting Information) and with the additive SRB (Figure 4a) in CLSM. However, the droplets are again only stable at high concentration, as the droplets dissolved upon dilution with water (Video S1 and Figure S11, Supporting Information) even though crosslinking was attempted. Nevertheless, in comparison to the noncrosslinked Pull-*b*-(PDMA-*co*-PDAAM), the crosslinked block copolymer features a high amount of small fluorescent particles even at lower concentration (at 10 wt%, Figure 4b). Thus, the crosslinking was not able to

stabilize the large separated phases. Albeit, the presence of smaller particles of lower concentration for crosslinked copolymer, signifies that crosslinking for Pull-*b*-(PDMA-*co*-PDAAM) takes place in a small area and not over the whole phase leaving crosslinked particles behind. Overall, even after crosslinking, the droplets at higher concentration are unstable.

As the state of phase separation could not be locked via crosslinking, we investigated the formed particle structures in more detail. In order to do so, the crosslinked Pull-*b*-(PDMA-*co*-PDAAM) was analyzed at lower concentration via DLS and cryo SEM (Figure 4c,d). An aqueous solution of 5.0, 2.4, 1.25, 0.6, and 0.1 wt% was investigated by DLS and the 0.6 wt% solution was analyzed via cryo SEM. The intensity weighted particle size distribution of crosslinked Pull-*b*-(PDMA-*co*-PDAAM) is dependent on the concentration (Figure S6 and Table S2, Supporting Information), which is similar to the noncrosslinked Pull-*b*-(PDMA-*co*-PDAAM). All concentrations show a trimodal particle size distribution. For more concentrated solutions, larger aggregates are visible. The small particles, with a peak around 5 nm for nearly all concentrations, can be attributed to the free block copolymer chains in the solution. The intensity of the free block copolymer chains increases, if the concentration decreases. The main peak is situated, dependent on the concentration, between 350 nm and 1.3 μm, which can be attributed to aggregate formation. In case of crosslinked block copolymer, the aggregates have a significant higher hydrodynamic radius than for noncrosslinked Pull-*b*-(PDMA-*co*-PDAAM). Dependent on the concentration, the hydrodynamic radius is two to four times larger than for the noncrosslinked Pull-*b*-(PDMA-*co*-PDAAM). Especially for the higher concentrated solutions (5.0 and 2.5 wt%), the hydrodynamic radius for the observed aggregates is larger, e.g., for 5 wt% solution (450 nm for noncrosslinked and 1.3 μm for crosslinked Pull-*b*-(PDMA-*co*-PDAAM)).

In order to underpin the results of DLS measurement, cryo SEM images of the 0.6 wt% solution of crosslinked block copolymer was recorded. The cryo SEM images display a significant amount of aggregates with a particle size in the range of 400 and 700 nm (Figure 4d). The average particle size, measured over 50 particles observed in the cryo SEM images (Figure S9, Supporting Information), is 581 nm with a standard deviation of 171 nm, which confirm the DLS results with a hydrodynamic radius of 367 nm for the larger aggregates in the 0.6 wt% solution. In comparison to the noncrosslinked Pull-*b*-(PDMA-*co*-PDAAM), the average particle size of the aggregates at a concentration of 0.6 wt% is around 60% higher for the crosslinked block copolymer. According to results of the DLS and cryo SEM measurements, it seems like the crosslinking of Pull-*b*-(PDMA-*co*-PDAAM) stabilized the aggregates of the block copolymer and further shifts the equilibrium to aggregates.

In order to remove free block copolymer chains in solution, the crosslinked Pull-*b*-(PDMA-*co*-PDAAM) was dialyzed against Millipore water for 3 days with MWCO 1000 kD. The dialyzed crosslinked block copolymer was analyzed via cryo SEM (Figure S12, Supporting Information) and DLS (Figure 3a and Table S3, Supporting Information). The results of DLS measurement possess a small peak around 10 nm. That peak could be derived from remaining free block copolymer chains in solution. Furthermore, the DLS measurement shows the main peak at 178 nm, which belongs to the larger aggregates.

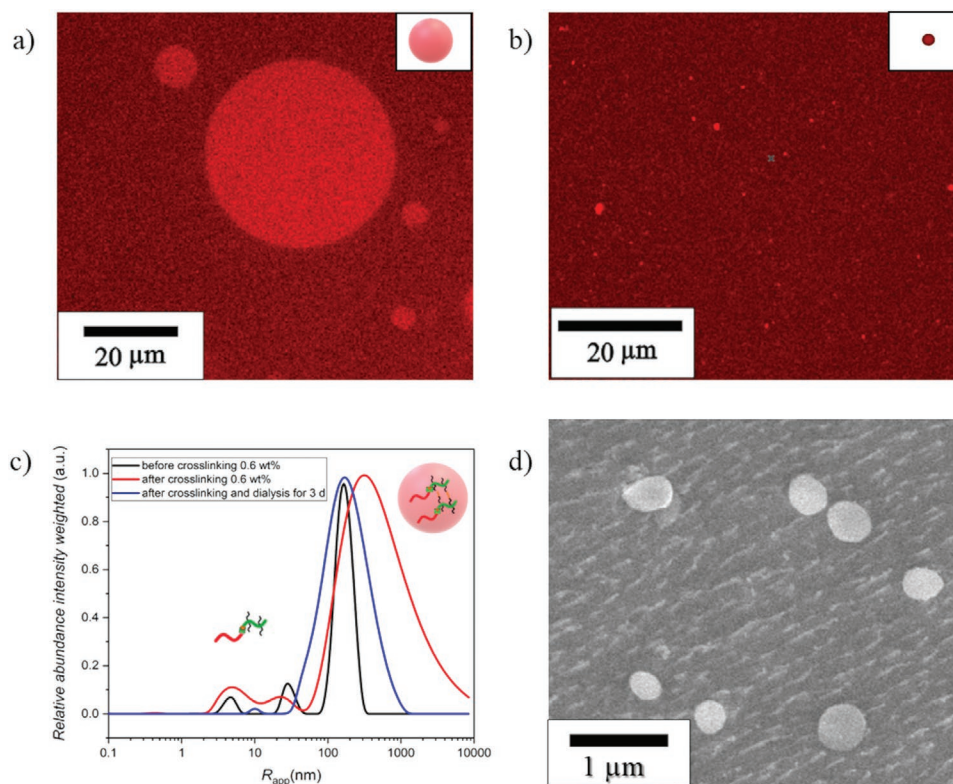


**Figure 4.** a) CLSM images of crosslinked Pull-*b*-(PDMA-*co*-PDAAM) at 20 wt% stained with Sulforhodamine B (SRB), b) CLSM images of crosslinked Pull-*b*-(PDMA-*co*-PDAAM) at 10 wt% stained with SRB, c) intensity weighted particle size distribution of 0.6 wt% solution of Pull-*b*-(PDMA-*co*-PDAAM) before (black curve) and after crosslinking (red curve), and crosslinked Pull-*b*-(PDMA-*co*-PDAAM) after dialysis against water for 3 days (blue curve) measured in water via DLS at 25 °C, d) cryo SEM images of Pull-*b*-(PDMA-*co*-PDAAM) crosslinking.

However, the results for the cryo SEM measurement display aggregates, which corresponding with the particle size to the DLS results (Table S3, Supporting Information). In addition, it shows aggregates, which are considerably larger than 1  $\mu\text{m}$  (Figure S12, Supporting Information) and significantly larger than the DLS results indicate, which could be due to considerable swelling of the particles at very low concentrations after dialysis. These structures resemble the structures observed by Brosnan et al. via cryo SEM.<sup>[23]</sup> Thus, the crosslinking stabilized the aggregates at lower concentration and these aggregates are larger in comparison to the noncrosslinked block copolymer. Overall, the crosslinking was successful to stabilize the aggregates at lower concentration but not strong enough to stabilize the polymer phase separation in the droplet state. A reason for that could be that the crosslinking does not take place over a longer distance in space and significant number of particles to stabilize the polymer phase separation but in a smaller area, therefore only small aggregates are observed at lower concentrated solution.

### 2.5. Aggregates of Crosslinked and Noncrosslinked Pull-*b*-(PDMA-*co*-PDAAM) in NMP

In order to prove the successful crosslinking of Pull-*b*-(PDMA-*co*-PDAAM) and the influence of the crosslinking for the stability of the aggregates in organic solvent, the block copolymer

was analyzed via DLS at 25 °C in *N*-methyl-2-pyrrolidone (NMP). For that, 1.0, 0.5, and 0.1 wt% solutions of the non-crosslinked and crosslinked block copolymer were investigated by DLS (Figure 5a and Table S4, Supporting Information) in NMP. For the noncrosslinked Pull-*b*-(PDMA-*co*-PDAAM), the results show a considerable dependency of stability on the polymer concentration. In the case of a low concentration, more larger particles are present in the solution and the intensity of smaller particles decreases for low concentration.

In contrast, the results for the crosslinked Pull-*b*-(PDMA-*co*-PDAAM) display no dependency on concentration. For all concentrations, the results are similar. Only the hydrodynamic radius of the larger aggregates increased at lower concentrated solutions, probably due to the swelling of the aggregates in the organic solvent. The smaller particles are all around 6 nm, with a similar intensity. The larger particles show an apparent average hydrodynamic radius between 252 and 375 nm. Especially for the low concentration, the results are similar to the DLS results for the crosslinked Pull-*b*-(PDMA-*co*-PDAAM) in water. In comparison to the noncrosslinked block copolymer, the crosslinked block copolymer shows no dependency on the concentration in an NMP solution. The significant difference of the DLS measurement shows that the crosslinking was successful, and it can stabilize the aggregates in low concentrated NMP solutions.

From the results, a simple scheme about the crosslinking process can be deduced (Scheme 2). At high concentrations

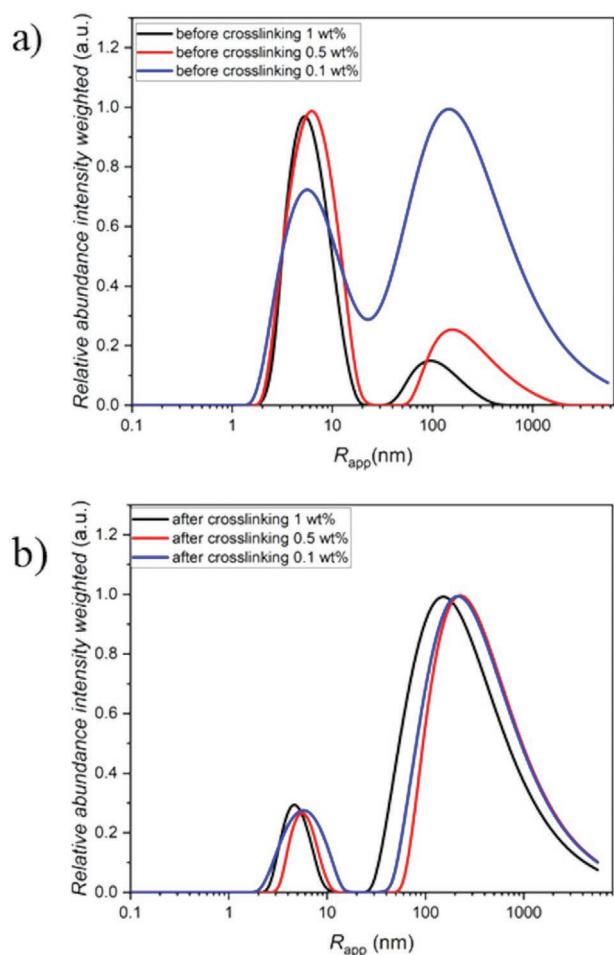


**Figure 5.** a,b) Comparison of intensity weighted particle size distribution of Pull-*b*-(PDMA-*co*-PDAAM) at different concentrations a) before and b) after crosslinking measured via DLS in NMP at 25 °C.

(20 wt%), a phase separation into polymer-enriched and polymer-depleted phases is present. In this case, dilution leads to dissolution of the separated phases. As crosslinking at high concentrations via oxime click chemistry is proceeding, the polymer-enriched phases are not crosslinked completely, and instead rather smaller areas within the phases are crosslinked. These crosslinked areas are preserved in the shape of particles after dissolution that are stable against dialysis (and very high dilution) and the organic solvent NMP.

### 3. Conclusion

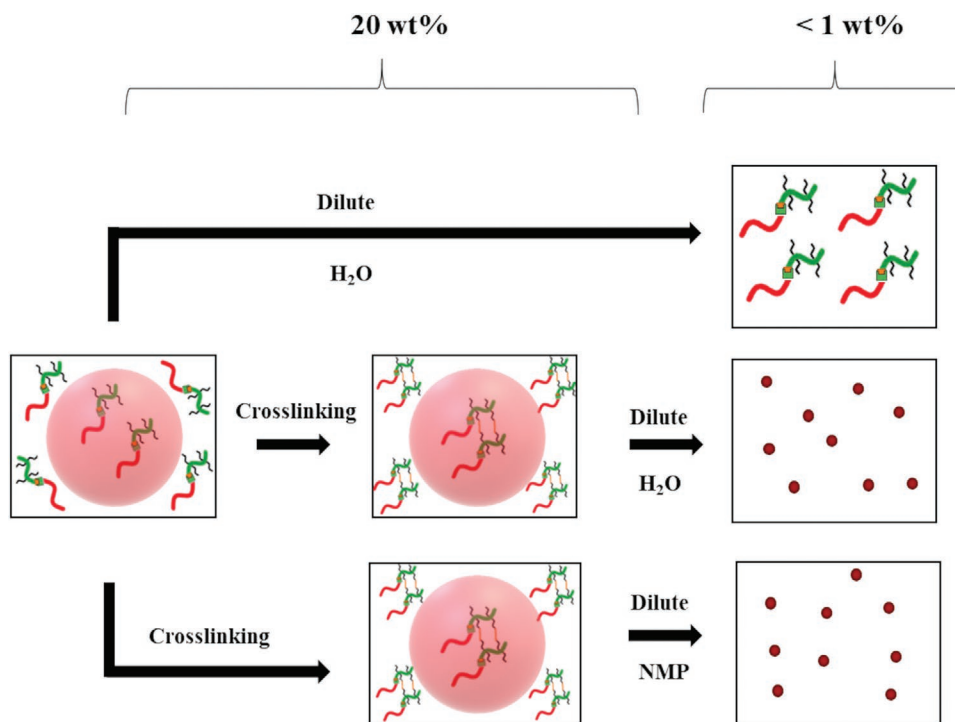
The DHBC Pull-*b*-(PDMA-*co*-PDAAM) was synthesized via CuAAC. The block copolymer shows mesoscale phase separation at high concentrations of 20 wt%, which is reversible upon dilution. In lower concentrated solution, Pull-*b*-(PDMA-*co*-PDAAM) displayed, dependently on the concentration, aggregates with sizes between 160 and 450 nm. Additionally, the Pull-*b*-(PDMA-*co*-PDAAM) was crosslinked via oxime formation. The crosslinked block copolymer induced droplet formation at high concentration of 20 wt% similar to the

noncrosslinked polymer. For lower concentrations, the crosslinked block copolymer featured aggregates with sizes between 350 nm and 1.3 μm. Furthermore, the crosslinked Pull-*b*-(PDMA-*co*-PDAAM) shows aggregates of around 1 μm, after dialysis against water. Studies in organic solvent showed an increased stability of the crosslinked aggregates of Pull-*b*-(PDMA-*co*-PDAAM) in low concentrated NMP solutions. By optimization of the stability of the aggregates at low concentrations, DHBCs might be interesting for biomedical applications.

### 4. Experimental Section

**Materials:** Acetone (99%, T.J Baker), ascorbic acid (98%, Alfa Aesar), azobis(isobutyronitrile) (AIBN, 99%, Sigma Aldrich, recrystallized from methanol), 1,3-bis(aminooxy)propan dihydrochloride (98%, Sigma Aldrich), 2-bromisobutyric acid (98%, Sigma Aldrich), 3-bromo-1-propanol (97%, Sigma Aldrich), carbon disulfide (CS<sub>2</sub>, 99%, Sigma Aldrich), copper sulfate (CuSO<sub>4</sub>, 99%, Carl Roth), *N,N'*-dicyclohexylcarbodiimide (DCC, 99%, Sigma Aldrich), 3,5-diaminobenzoic acid dihydrochloride (DABA, 98%, may contain up to 3% moisture, Alfa Aesar), *N,N*-dimethylacrylamide (DMA, 99%, TCI, passed over a column of neutral aluminum oxide), 4-dimethylaminopyridine (DMAP, 99%, Sigma Aldrich), *N,N*-dimethylformamide (DMF, analytical grade, VWR), dimethylsulfoxide (DMSO, analytical grade, VWR Chemicals), *N*-(1,1-dimethyl-3-oxobutyl)acrylamide (99%, Sigma Aldrich), dodecanethiol (98%, Alfa Aesar), *N*-methyl-2-pyrrolidone (NMP, Fluka, GC grade), Millipore water (obtained from an Integra UV plus pure water system by SG Water (Germany)), *N,N,N',N'',N''*-pentamethyldiethylenetriamine (PMDETA, 98%, Sigma Aldrich), potassium phosphate (K<sub>3</sub>PO<sub>4</sub>, Sigma Aldrich), propargylamine (98%, Sigma Aldrich), pullulan (Pull, pure, TCI), Rhodamine B isothiocyanate (RITC, 99%, Sigma Aldrich), sodium azide (99.5% Fluka), sodium cyanoborohydride (NaCNBH<sub>3</sub>, 95%, Sigma Aldrich), Sulforhodamine B (Sigma Aldrich), tetrahydrofuran (THF, extra dry, Acros Organics), and triethylamine (99.5%, Sigma Aldrich). Dodecylthiocarbonylthio-2-methylpropanoic acid 3'-azido propyl ester and azido functionalized PS-resin were synthesized according to the literature.<sup>[30,50]</sup> Pullulan was depolymerized<sup>[61]</sup> and alkyne end-functionalized<sup>[62]</sup> according to the literature. The coupling of the two blocks was conducted via azide-alkyne cycloaddition based on the work of Bernard et al.<sup>[47]</sup>

**Analytical Methods:** <sup>1</sup>H-NMR spectra were recorded in deuterium oxide (D<sub>2</sub>O, Aldrich) at ambient temperature at 400 MHz with a Bruker Ascend400 or at 600 MHz with an Agilent600. <sup>13</sup>C spectra were recorded in deuterium oxide (D<sub>2</sub>O, Aldrich) at 600 MHz with an Agilent600. DOSY was performed in deuterated dimethylsulfoxide (DMSO-*d*<sub>6</sub>, Aldrich) at 600 MHz with an Agilent600 using the Dbppste\_CC pulse sequence. Dynamic light scattering (DLS) was performed using an ALV-7004 Multiple Tau Digital Correlator in combination with a CGS-3 Compact Goniometer and a HeNe laser (Polytec, 34 mW, λ = 633 nm at θ = 90° setup for DLS). Toluene was used as immersion liquid and sample temperatures were adjusted to 25 °C. Apparent hydrodynamic radii (*R*<sub>app</sub>) were determined from fitting autocorrelation functions using the CONTIN algorithm. Cryogenic scanning electron microscopy (cryo SEM) was conducted with a Jeol JSM 7500 F and the cryo-chamber from Gatan (Alto 2500). The average particle size of the 0.6 wt% solution of Pull-*b*-PDMA-*co*-PDAAM before and after crosslinking was measured over 50 particles in cryo SEM pictures. The error bar is based on the standard deviation. Size exclusion chromatography (SEC) of pullulan and acrylamides was conducted in acetate buffer containing 20% methanol with the salt peak as internal standard at 25 °C using a column system with a PSS Suprema VS; PSS Suprema 10 μm, 30 Å; PSS Suprema 10 μm and PSS SECURITY Refractive Index-1260 RID and calibrated with pullulan standards. Confocal laser scanning microscopy (CLSM) was performed on a Leica TCS SP5 (Wetzlar, Germany) confocal microscope, using a 63 × (1.2 NA) water immersion objective. Labelled polymer and SRB were



**Scheme 2.** Overview of the observed aggregation of Pull-*b*-(PDMA-*co*-PDAAM) and crosslinked Pull-*b*-(PDMA-*co*-PDAAM).

excited with a diode pumped solid-state laser at 561 nm, and emission was detected at 565–620 nm. Images were acquired at  $512 \times 512$  pixels at 400 Hz scanning speed with 1–2 line averages.

**Formation of PDMA-*co*-PDAAM:** In a dry, argon purged 100 mL round bottom Schlenk flask, dodecylthiocarbonylthio-2-methylpropanoic acid 3'-azidopropylester (40.8 mg, 0.1 mmol, 1 eq.), AIBN (3.0 mg, 0.018 mmol, 0.2 eq.), DMA (1.8 g, 18.16 mmol, 181.6 eq.), and *N*-(1,1-dimethyl-3-oxobutyl)acrylamide (0.77 g, 4.54 mmol, 45.4 eq.) were dissolved in DMF (5.6 mL). The solution was degassed by three freeze-pump-thaw cycles and placed in a pre-heated oil bath (60 °C). Subsequently, the reaction mixture was stirred for 6 h, stopped by cooling down with liquid nitrogen and exposure to air. Afterward, the polymer was dialyzed against deionized water (Spectra/Por 3500 Da) for three days, freeze-dried and a yellow solid (2.14 g,  $M_n = 21800 \text{ g mol}^{-1}$ ,  $D = 1.9$  measured in acetate buffer against pullulan standards) was obtained.

**RAFT Group Removal of PDMA-*co*-PDAAM:** According to the literature,<sup>[59]</sup> in a 100 mL round bottom flask, AIBN (0.364 g, 2.15 mmol, 40 eq.) was dissolved in destabilized THF (120 mL). The solution was stirred vigorously for 30 min at 60 °C under air. After a positive peroxide test, PDMA-*co*-PDAAM (1.5 g, 0.054 mmol, 1.0 eq.) was added. The reaction mixture was stirred at 60 °C, until the yellow color vanished. Subsequently, the reaction was cooled down to ambient temperature and the THF was removed under reduced pressure. The remaining crude product was dissolved in deionized water, dialyzed against deionized water (Spectra/Por 3500 Da) for three days, freeze-dried and a slightly greenish solid (1.32 g,  $M_n = 21800 \text{ g mol}^{-1}$  measured in acetate buffer against pullulan standards) was obtained.

**Formation of Pull-*b*-(PDMA-*co*-PDAAM):** Pullulan-alkyne (0.52 g, 0.028 mmol, 1.2 eq.) was dissolved in Millipore water (7.5 mL).  $\text{CuSO}_4$  (2.4 mg, 0.015 mmol, 0.65 eq.), DMSO (10 mL), ascorbic acid (8.1 mg, 0.046 mmol, 2 eq. in 2.5 mL water), PMDETA (6 mg, 0.035 mmol, 1.5 eq. in 5 mL DMSO), and PDMA-*co*-PDAAM (0.5 g, 0.023 mmol, 1 eq.) were added to the solution. The reaction mixture was stirred for two days at ambient temperature. Ascorbic acid (8.1 mg) and azido functionalized PS-resin (16 mg) was added to the reaction mixture and was stirred

for two days at ambient temperature. Subsequently, the polymer was dialyzed against deionized water (Spectra/Por 3500 Da). Finally, the sample was freeze-dried and a white solid (0.98 g,  $M_n = 25300 \text{ g mol}^{-1}$  measured in acetate buffer against pullulan standards) was obtained. For Rhodamine B labelled Pull-*b*-(PDMA-*co*-PDAAM), the copolymer PDMA-*co*-PDAAM was synthesized in a similar way and subsequently conjugated with RITC (refer to the ESI<sup>†</sup> for details).

**Crosslinking of Pull-*b*-(PDMA-*co*-PDAAM):** Pull-*b*-(PDMA-*co*-PDAAM) (0.1 g, 0.004 mmol, 1.0 eq.) was dissolved in Millipore water (0.4 mL, all used Millipore water was filtered with a  $0.45 \mu\text{m}$  CA syringe filter). 1,3-bis(aminoxy)propan dihydrochloride (26  $\mu\text{L}$ , 0.0002 mmol, 0.05 eq. from a aqueous stock solution 1.4 mg in 1 mL Millipore water), DABA (1  $\mu\text{L}$ , from an aqueous stock solution 1 mg in 1 mL Millipore water) and triethylamine (23  $\mu\text{L}$ , 0.008 mmol, 0.2 eq. from a aqueous stock solution 1  $\mu\text{L}$  in 200  $\mu\text{L}$  Millipore water) was added to the polymer solution. The reaction mixture was placed in a 35 °C oil-bath overnight.

**Analysis of Pull-*b*-(PDMA-*co*-PDAAM):** A 5 wt% solution of Pull-*b*-(PDMA-*co*-PDAAM) was diluted with Millipore water (filtered with a  $0.45 \mu\text{m}$  CA syringe filter) to 2.5, 1.25, 0.6, and 0.1 wt% for DLS characterization. Cryo SEM was performed with a 0.6 wt% solution.  $^1\text{H-NMR}$  and  $^{13}\text{C-NMR}$  were conducted with freeze dried samples.

**Analysis of Crosslinked Pull-*b*-(PDMA-*co*-PDAAM):** A 5 wt% solution of crosslinked Pull-*b*-(PDMA-*co*-PDAAM) was diluted with Millipore water (filtered with a  $0.45 \mu\text{m}$  CA syringe filter) to 2.5, 1.25, 0.6, and 0.1 wt% for DLS characterization. 2.5 wt% (2 mL) and 1.25 wt% (2 mL) polymer solution were combined and dialyzed against Millipore water (Spectra/Por 1000 kDa) and analyzed via DLS and cryo SEM. The 0.6 wt% solution was analyzed via cryo SEM.  $^1\text{H-NMR}$  and  $^{13}\text{C-NMR}$  were conducted with freeze dried samples.

## Supporting Information

Supporting Information is available from the Wiley Online Library or from the author.

## Acknowledgements

The authors thank the Max-Planck society and the Deutsche Forschungsgemeinschaft (DFG) (SCHM 3282/3-1) for funding. The authors acknowledge Marlies Gräwert for SEC measurements and Heike Runge for assistance with cryogenic SEM.

## Conflict of Interest

The authors declare no conflict of interest.

## Keywords

biopolymers, block copolymers, crosslinking, reversible addition fragmentation chain transfer (RAFT), self-assembly

Received: February 10, 2020

Revised: May 6, 2020

Published online:

- [1] M. A. C. Stuart, W. T. Huck, J. Genzer, M. Müller, C. Ober, M. Stamm, G. B. Sukhorukov, I. Szleifer, V. V. Tsukruk, M. Urban, *Nat. Mater.* **2010**, 9, 101.
- [2] X. Qiang, R. Chakroun, N. Janoszka, A. H. Gröschel, *Isr. J. Chem.* **2019**, 59, 945.
- [3] D. Schmaljohann, *Adv. Drug Delivery Rev.* **2006**, 58, 1655.
- [4] R. Langer, *Nature* **1998**, 392, 5.
- [5] K. T. Kim, J. J. Cornelissen, R. J. Nolte, J. C. van Hest, *Adv. Mater.* **2009**, 21, 2787.
- [6] J. Jagur-Grodzinski, *Polym. Adv. Technol.* **2006**, 17, 395.
- [7] M.-C. Jones, J.-C. Leroux, *Eur. J. Pharm. Biopharm.* **1999**, 48, 101.
- [8] D. E. Discher, A. Eisenberg, *Science* **2002**, 297, 967.
- [9] B. M. Discher, Y.-Y. Won, D. S. Ege, J. C. Lee, F. S. Bates, D. E. Discher, D. A. Hammer, *Science* **1999**, 284, 1143.
- [10] J. S. Lee, J. Feijen, *J. Controlled Release* **2012**, 161, 473.
- [11] P. Tanner, P. Baumann, R. Enea, O. Onaca, C. Palivan, W. Meier, *Acc. Chem. Res.* **2011**, 44, 1039.
- [12] B. V. K. J. Schmidt, *Macromol. Chem. Phys.* **2018**, 219, 1700494.
- [13] G. Li, S. Song, L. Guo, S. Ma, *J. Polym. Sci., Part A: Polym. Chem.* **2008**, 46, 5028.
- [14] Z. Ge, D. Xie, D. Chen, X. Jiang, Y. Zhang, H. Liu, S. Liu, *Macromolecules* **2007**, 40, 3538.
- [15] A. Rösler, G. W. Vandermeulen, H.-A. Klok, *Adv. Drug Delivery Rev.* **2012**, 64, 270.
- [16] Y. Mai, A. Eisenberg, *Chem. Soc. Rev.* **2012**, 41, 5969.
- [17] C. R. Mace, O. Akbulut, A. A. Kumar, N. D. Shapiro, R. Derda, M. R. Patton, G. M. Whitesides, *J. Am. Chem. Soc.* **2012**, 134, 9094.
- [18] J. Zhang, J. Hwang, M. Antonietti, B. V. Schmidt, *Biomacromolecules* **2019**, 20, 204.
- [19] Y. Liu, R. Lipowsky, R. Dimova, *Front. Chem.* **2019**, 7, 213.
- [20] R. Dimova, R. Lipowsky, *Adv. Mater. Interfaces* **2017**, 4, 1600451.
- [21] J. Wu, Z. Wang, Y. Yin, R. Jiang, B. Li, A.-C. Shi, *Macromolecules* **2015**, 48, 8897.
- [22] A. Blanz, N. J. Warren, A. L. Lewis, S. P. Armes, A. J. Ryan, *Soft Matter* **2011**, 7, 6399.
- [23] S. M. Brosnan, H. Schlaad, M. Antonietti, *Angew. Chem., Int. Ed.* **2015**, 54, 9715.
- [24] O. Casse, A. Shkillyny, J. r. Linders, C. Mayer, D. Häussinger, A. Völkel, A. F. Thünemann, R. Dimova, H. Cölfen, W. Meier, *Macromolecules* **2012**, 45, 4772.
- [25] A. Taubert, E. Furrer, W. Meier, *Chem. Commun.* **2004**, 2170.
- [26] F. Ke, X. Mo, R. Yang, Y. Wang, D. Liang, *Macromolecules* **2009**, 42, 5339.
- [27] J. Willersinn, B. V. K. J. Schmidt, *Polymers* **2017**, 9, 293.
- [28] T. Rudolph, S. Crotty, M. von der Lühe, D. Pretzel, U. Schubert, F. Schacher, *Polymers* **2013**, 5, 1081.
- [29] J. Willersinn, B. V. K. J. Schmidt, *Polym. Chem.* **2018**, 9, 1626.
- [30] J. Willersinn, A. Bogomolova, M. B. Cabré, B. V. K. J. Schmidt, *Polym. Chem.* **2017**, 8, 1244.
- [31] H. Park, S. Walta, R. Rosencrantz, A. Körner, C. Schulte, L. Elling, W. Richtering, A. Böker, *Polym. Chem.* **2016**, 7, 878.
- [32] T. Oh, M. Nagao, Y. Hoshino, Y. Miura, *Langmuir* **2018**, 34, 8591.
- [33] J. Quan, F.-W. Shen, H. Cai, Y.-N. Zhang, H. Wu, *Langmuir* **2018**, 34, 10721.
- [34] A. Adharis, T. Ketelaar, A. G. Komarudin, K. Loos, *Biomacromolecules* **2019**, 20, 1325.
- [35] L. Chen, X. Wang, F. Ji, Y. Bao, J. Wang, X. Wang, L. Guo, Y. Li, *RSC Adv.* **2015**, 5, 94719.
- [36] I. W. Sutherland, *Trends Biotechnol.* **1998**, 16, 41.
- [37] R. S. Singh, N. Kaur, J. F. Kennedy, *Carbohydr. Polym.* **2015**, 123, 190.
- [38] V. D. Prajapati, G. K. Jani, S. M. Khanda, *Carbohydr. Polym.* **2013**, 95, 540.
- [39] W. M. Kulicke, T. Heinze, *Macromol. Symp.* **2005**, 231, 47.
- [40] H. Hosseinkhani, T. Aoyama, O. Ogawa, Y. Tabata, *J. Controlled Release* **2002**, 83, 287.
- [41] M. Rekha, C. P. Sharma, *Trends Biomater. Artif. Organs* **2007**, 20, 116.
- [42] A. B. Lowe, C. L. McCormick, *Prog. Polym. Sci.* **2007**, 32, 283.
- [43] R. Huisgen, G. Szeimies, L. Möbius, *Chem. Ber.* **1967**, 100, 2494.
- [44] H. C. Kolb, K. B. Sharpless, *Drug Discovery Today* **2003**, 8, 1128.
- [45] K. Kempe, A. Krieg, C. R. Becer, U. S. Schubert, *Chem. Soc. Rev.* **2012**, 41, 176.
- [46] J. F. Lutz, *Angew. Chem., Int. Ed.* **2007**, 46, 1018.
- [47] J. Bernard, M. Save, B. Arathoon, B. Charleux, *J. Polym. Sci., Part A: Polym. Chem.* **2008**, 46, 2845.
- [48] H. Gao, K. Matyjaszewski, *J. Am. Chem. Soc.* **2007**, 129, 6633.
- [49] A. Gregory, M. H. Stenzel, *Prog. Polym. Sci.* **2012**, 37, 38.
- [50] S. R. Gondi, A. P. Vogt, B. S. Sumerlin, *Macromolecules* **2007**, 40, 474.
- [51] R. K. O'Reilly, C. J. Hawker, K. L. Wooley, *Chem. Soc. Rev.* **2006**, 35, 1068.
- [52] N. Al Nakeeb, J. Willersinn, B. V. K. J. Schmidt, *Biomacromolecules* **2017**, 18, 3695.
- [53] N. Al Nakeeb, Z. Kochovski, T. Li, Y. Zhang, Y. Lu, B. V. K. J. Schmidt, *RSC Adv.* **2019**, 9, 4993.
- [54] N. Al Nakeeb, I. Nischang, B. V. K. J. Schmidt, *Nanomaterials* **2019**, 9, 662.
- [55] G. N. Grover, J. Lam, T. H. Nguyen, T. Segura, H. D. Maynard, *Biomacromolecules* **2012**, 13, 3013.
- [56] S. Mukherjee, A. P. Bapat, M. R. Hill, B. S. Sumerlin, *Polym. Chem.* **2014**, 5, 6923.
- [57] J. Collins, Z. Xiao, M. Müllner, L. A. Connal, *Polym. Chem.* **2016**, 7, 3812.
- [58] M. B. Sims, K. Y. Patel, M. Bhatta, S. Mukherjee, B. S. Sumerlin, *Macromolecules* **2018**, 51, 356.
- [59] B. V. K. J. Schmidt, C. Barner-Kowollik, *Polym. Chem.* **2014**, 5, 2461.
- [60] M. Dietrich, M. Glassner, T. Gruending, C. Schmid, J. Falkenhagen, C. Barner-Kowollik, *Polym. Chem.* **2010**, 1, 634.
- [61] L. Ilić, K. Jeremić, S. Jovanović, *Eur. Polym. J.* **1991**, 27, 1227.
- [62] C. Schatz, S. Louguet, J. F. Le Meins, S. Lecommandoux, *Angew. Chem., Int. Ed.* **2009**, 48, 2572.
- [63] K. Nicolay, K. P. Braun, R. A. d. Graaf, R. M. Dijkhuizen, M. J. Kruiswijk, *NMR Biomed.* **2001**, 14, 94.
- [64] R. B. Lira, J. Willersinn, B. V. K. J. Schmidt, R. Dimova, **2020**, unpublished.
- [65] P. Crisalli, E. T. Kool, *J. Org. Chem.* **2013**, 78, 1184.